Definition of the profile gain factor and its application for internal transport barrier analysis in torus plasmas

Definition of the profile gain factor and its application for internal transport barrier analysis in torus plasmas

T. Kobayashi[1,2], H. Takahashi[1,2], K. Nagaoka[1], M. Sasaki[3,4], M. Yokoyama[1,2], R. Seki[1,2], M. Yoshinuma[1], K. Ida[1], and LHD Experiment Group

[1] National Institute for Fusion Science, National Institutes of Natural Sciences, Toki 509-5292, Japan

[2] SOKENDAI (The Graduate University for Advanced Studies), Toki 509-5292, Japan

[3] Research Institute for Applied Mechanics, Kyushu University, Kasuga 816-8580, Japan

[4] Research Center for Plasma Turbulence, Kyushu University, Kasuga 816-8580, Japan

E-mail: kobayashi.tatsuya@nifs.ac.jp

Abstract. In this paper, a new criterion for the internal transport barrier formation is proposed by defining a unique scalar parameter, the profile gain factor. The profile gain factor shows degree of the confinement improvement with respect to an arbitrary reference temperature profile scaling in the L-mode. As the reference L-mode profile for the Large Helical Device (LHD), the edge ion temperature profile data is extrapolated to the core by the L-mode profile function, which uses the thermal diffusion coefficient being proportional to the local ion temperature. The profile gain factor is defined as the ratio of the ion stored energy experimentally measured to that evaluated from the reference L-mode profile. The proposed method is applied to the LHD experimental data, and its capability for quantification of the ITB strength is demonstrated.

1. Introduction

It is widely known that the more heating power is applied the worse the plasma confinement becomes in magnetically confined plasmas. This is the so-called power degradation problem. Because of this issue, a large heating facility is expected to be necessary for realizing the self-ignition condition in thermonuclear fusion reactors, which can be one of the crucial difficulties for building commercial plants. A possible breakthrough was the discovery of confinement improved scenarios [1, 2, 3], including the H-mode discharges and the internal transport barrier (ITB) discharges. These discharges typically have an eased power degradation, which contributes to make plasmas having a good performance. To utilize such scenarios in actual fusion plants, it is mandatory to understand the background physics for establishing schemes to control discharges with improved confinement mode.

The first step to investigate the improved confinement mode is to give a proper definition for these modes. A successful example can be seen in the case of the H-mode [3]. The H-mode discharges are typically characterized by a sudden drop in the H_α (D_α) emission from the scrape off layer or divertor regions showing suppressed turbulent particle flux. Steep gradients emerge in the temperature and density profiles, which are called the pedestal structure. Because of its relatively clear hard transition feature, the criterion of the H-mode transition is definitely given and several key underlying physics are clarified, such as essential role of the radial electric field structure, turbulent transport reduction, and density dependent threshold power that also has isotope ion

mass dependence.

In contrast, regarding the ITB, in particular the ITB in the ion temperature profile, no generally accepted definition exists. The literal definition of the ITB is that the confinement is improved inside the plasma. This definition is too vague to utilize for the quantification of the ITB. In addition, there are a wide variety of the ITBs that have different degrees of confinement improvement [2], ranging from 'box-type' strong ITBs in the reversed shear configuration to moderate ITBs in stellarators/heliotrons, which makes unification of criterions difficult to achieve. In cases of the strong ITB, localized reduction of transport can easily be identified merely by plotting the temperature gradient or the diffusion coefficient [4, 5, 6]. A widely used criterion in tokamaks is whether the major radius divided by the temperature gradient length, R/L_T, exceeds the critical value [1, 7, 8, 9]. This idea originates from the tokamak L-mode profile that has stiffness [10, 11]; R/L_T above the critical value manifests the situation where the plasma overcomes the restriction of the profile stiffness. In stellarators/heliotrons the temperature profile is not stiff in many cases [12, 13]. Therefore, the validity of R/L_T for the ITB criterion in stellarators/heliotrons is questionable.

Another criterion of the ITB is given by observing the temperature T dependence of the thermal diffusion coefficient χ. The parameter α is defined as $\alpha = -d\chi/dT$, and the case $\alpha < 0$ is regarded to be the ITB [14, 15, 16]. In contrast, the L-mode plasmas have $\alpha > 0$, which is consistent with the incrementally scaled temperature dependence of the energy confinement time in the Bohm scaling or the gyro-Bohm scaling. When

$\alpha > 0$, the more the temperature increases the worse the confinement becomes, bringing the typical profile shape that has flatter gradient in the core region and steeper gradient at the edge region. This constraint is violated when the ITB is formed. Besides the direct quantification of the α parameter [14, 15, 16], the temperature gradient ratio between the core region and the edge region was employed as an ITB criterion [17]. Although these criterions are based on the essential physics of the ITB, it is necessary to make detailed discussions on the profiles of χ or $-\nabla T$ for each time step, which is often laborious. Therefore, these criterions are not always applicable in particular for a large database with a wide range parameter scan experiment. Moreover, the direct use of the temperature gradient can be an error source in the case that the measurement noise in the temperature profile is not negligibly small.

In this paper, we propose a new criterion of the ITB confinement improvement by defining a unique scalar parameter, the profile gain factor. The profile gain factor quantifies degree of the confinement improvement with respect to an arbitrary reference temperature profile scaling in the L-mode. As a case study, we analyze the ion temperature profile in Large Helical Device (LHD). The L-mode ion temperature profiles in LHD are characterized by the dome-shaped profile, where the confinement degrades as the ion temperature increases towards the core [17]. The function form of the L-mode profile, the so-called the L-mode profile function, is derived for the dome-shaped ion temperature profile. Whether the ITB is formed or not is discussed based on the fact that the confinement scaling of the ITB is similar to that of the L-mode in the edge

region [1]. Edge ion temperature profile data is fitted by the L-mode profile function, and is extrapolated to the core keeping the same scaling manner, which is called the reference L-mode profile. When the core confinement is attributed to the ITB, the measured ion temperature profile deviates from the reference L-mode profile, while both become similar in the L-mode phase. The profile gain factor is defined as the ratio of the ion stored energy experimentally measured to that evaluated from the reference L-mode profile. The proposed method is applied to the measured data in LHD, and its capability for quantification of the ITB strength is demonstrated.

This paper is organized as follows. In section 2, the L-mode profile function and the profile gain factor are derived. Note that the discussion given in sections 2 is valid for both ions and electrons, therefore we do not specify the target species. Application of the profile gain factor for the ion temperature profiles in the LHD experimental data is presented in section 3. The contents given in this paper are summarized in section 4. Detailed numerical schemes for solving the nonlinear thermal transport equation are given with a simple numerical test in Appendix.

2. Derivation of the L-mode profile function and the profile gain factor

The L-mode profile function is derived from the steady-state thermal transport equation for any particle species,

$$0 = -\frac{1}{V'}\frac{\partial}{\partial r}\left(V'q\right) + P, \tag{1}$$

where q is the radial heat flux, n is the density, $V' = \partial V/\partial r$ is the partial derivative

of the volume enclosed by the flux surface with respect to the flux surface coordinate r, and P is the heating power density that includes the energy exchange with other species. The profile gain factor can be defined when q of the typical L-mode plasma can be modeled as a function of the temperature T, its radial derivative $\partial T/\partial r$, and some constant parameters, and when Eq. (1) can be numerically solved with the model of q under given experimental parameters, n, V', and P. In the case of the LHD, it is empirically known that both the ion and electron temperature profiles in the L-mode become the dome-shaped profile, which can be modeled by the pure diffusion equation with the diffusion coefficient incrementally scaling with the local temperature. Therefore, the radial heat flux can be given as

$$q = -n\chi\frac{\partial T}{\partial r}, \tag{2}$$

where χ is the thermal diffusion coefficient. The nonlinear dependence of χ on T is represented as

$$\chi = kT^{\alpha}, \tag{3}$$

where α is a parameter that shows how strong the diffusion coefficient depends on the temperature and k is the proportionality factor. Note that the temperature dependences on the global energy confinement time in the Bohm scaling and the gyro-Bohm scaling correspond to $\alpha = 1$ and 1.5, respectively. The global energy confinement time scaling in LHD derived from a wide range parameter scan approximately follows the gyro-Bohm scaling [18]. The temperature profile in the L-mode is not always characterized by Eqs. (2) and (3) in other devices. For example, it is widely known that the L-mode

temperature profile in tokamaks shows the profile stiffness [10, 11], in which the dome-shaped profile does not appear. In such a case, it is necessary to derive the model of q and the scaling property of the transport coefficients for calculating the profile gain factor. The thermal transport equation now becomes

$$kT^{\alpha}\left[\frac{\partial^2 T}{\partial r^2}+\frac{1}{L}\frac{\partial T}{\partial r}+\frac{\alpha}{T}\left(\frac{\partial T}{\partial r}\right)^2\right]+\frac{P}{n}=0. \tag{4}$$

The specific scale length L is defined as

$$\frac{1}{L}=\frac{1}{L_n}+\frac{1}{L_{V'}}, \tag{5}$$

where

$$\frac{1}{L_n}=\frac{1}{n}\frac{\partial n}{\partial r} \tag{6}$$

and

$$\frac{1}{L_{V'}}=\frac{1}{V'}\frac{\partial V'}{\partial r} \tag{7}$$

are the inverse scale lengths of the density profile and the the partial derivative of the torus volume profile, respectively. When the flux surface coordinate is defined as $r=\sqrt{V/2\pi^2 R_0}$, where R_0 is a characteristic major radius, $L_{V'}^{-1}=r^{-1}$ holds. The nonlinear partial differential equation is solved numerically for given parameters k and α. The solution is obtained iteratively by use of the Levenberg-Marquardt method. See Appendix for details.

Now the temperature profile that satisfies Eq. (4) is regarded to be a function of k and α, namely,

$$T(r)=T(r|k,\alpha). \tag{8}$$

In addition, as will be shown below, the ion temperature profile in the typical L-mode phase can be well fitted with $\alpha = 1$ in the case of the present LHD data. Accordingly, Eq. (8) with $\alpha = 1$, i.e.,

$$T(r) = T(r|k) \tag{9}$$

is called the L-mode profile function. Whether the ITB is formed or not is discussed based on the fact that the confinement scaling of the ITB is similar to that of the L-mode in the edge region [1]. The parameter k of $T_{\rm L}(r|k)$ is obtained from the measured temperature profile in the edge region by the nonlinear fitting, and the entire temperature profile is recreated by extrapolating $T_{\rm L}(r|k)$ to the core. This recreated profile is called the reference L-mode profile $T_{\rm L}^{\rm ref}(r)$, and corresponds to the temperature profile that is expected to appear when the confinement is determined by the L-mode scaling. Another Levenberg-Marquardt least square fitting is used for obtaining k with numerically evaluated Jacobian matrix. The radial range for the nonlinear fitting is called the fitting range, in which the ITB profile has the same scaling manner with the typical L-mode profile. How much the measured temperature profile exceeds the reference L-mode profile is used as the criterion of the ITB confinement improvement. To quantify this discrepancy, the profile gain factor is defined as

$$G_\alpha = \frac{\int_0^a nT(r)V'dr}{\int_0^a nT_{\rm L}^{\rm ref}(r)V'dr}, \tag{10}$$

where a is the plasma minor radius and the subscript α denotes the α parameter employed for the L-mode profile function. The numerator corresponds to the kinetic plasma energy stored in the species of interest, and the denominator is that with respect

to the obtained reference L-mode profile. The profile gain factor measures degree of the confinement improvement with respect to the reference L-mode profile inside the fitting range. By use of the profile gain factor, the confinement property in the core region can be investigated separately from that in the edge region, e.g., the edge pedestal structure.

3. Application for experimental data

3.1. Experimental setup

The method proposed above is applied to the analysis of the ion temperature profile dynamics in LHD. The target plasmas are produced by the five high intensity neutral beams (NBs) above 20 MW in total. The confinement field is $B_{\rm t} = 2.85$ T in the counter clockwise direction observed from the top side of the torus. The magnetic axis in the vacuum configuration is $R_{\rm ax} = 3.6$ m. The ion temperature profile $T_{\rm i}$ is measured by the charge exchange recombination spectroscopy for the carbon impurity emission [19]. The electron temperature profile $T_{\rm e}$ and the electron density profile $n_{\rm e}$ are given by the Thomson scattering system [20]. Spatial resolutions of these two profile measurement systems are high enough to discuss the profile gain factor. The energy exchange between ions and electrons, $P_{\rm ie}$, is proportional to the difference between the ion temperature and the electron temperature. The heat deposition of the NB $P_{\rm NB}$ is evaluated by the beam simulation code FIT3D [21]. The radial derivative of the plasma volume V' is given from the equilibrium calculation code. In LHD, the effective minor radius $r_{\rm eff}$ is conventionally used as the flux surface coordinate, i.e., the radial coordinate. The

plasma edge is defined by the averaged minor radius in which 99 % of the plasma kinetic energy is confined, to be $a_{99} \sim 0.63$ m. In this paper data from two different discharges, i.e., the stationary L-mode discharge and the ion-ITB transition discharge, are analyzed for demonstrating the usefulness of the profile gain factor in ion-ITB formation study.

3.2. Analysis of the stationary L-mode discharge

At first, the profile gain factor is evaluated for the case of the L-mode discharge. Empirically, the ITB is formed in the low density regime with sufficiently high NB power input. Therefore, the high density discharge with the line averaged electron density of $\sim 3 \times 10^{19}$ m^{-3} is chosen as the typical L-mode discharge. The present data is from the discharge # 141189 at the time frame of $t = 3.95$ s. The radial profiles of the plasma parameters are shown in Figs. 1 (a)-(c). The instant diffusion coefficient is defined as $\chi_{\rm i} = q_{\rm i}/n_{\rm e}|\nabla T_{\rm i}|$, where the ion heat flux $q_{\rm i}$ is given by the power balance analysis, i.e., $q_{\rm i} = V'^{-1}\int_0^r (P_{\rm NB} + P_{\rm ie})V'dr$. The radial derivative for $\nabla T_{\rm i}$ is taken after performing the second order Bessel function smoothing to reduce noise. The diffusion coefficient $\chi_{\rm i}$ is plotted as a function of $T_{\rm i}$ for various radii in Fig. 1 (d) to experimentally obtain the α parameter. The points in $r_{\rm eff} \leq 0.1$ m and $r_{\rm eff} \geq 0.55$ m are not shown because noise is large and the gradient is not properly evaluated. All the plotted points are approximately aligned on a linear line, showing that Eq. (3) with $\alpha = 1$ represents the ion temperature dependence of the diffusion coefficient. The ion temperature profile experimentally measured in the fitting range of $0.45 \leq r_{\rm eff} \leq 0.55$ m

is fitted by $T_{\mathrm{i,L}}(r|k)$ to obtain the parameter k. The L-mode profile function $T_{\mathrm{i,L}}(r|k)$ with the obtained k parameter is extrapolated to the core, which is called the reference L-mode profile $T_{\mathrm{i,L}}^{\mathrm{ref}}(r)$. The red curve in Fig. 1 (a) corresponds to $T_{\mathrm{i,L}}^{\mathrm{ref}}(r)$. It is shown that the measured ion temperature profile is well reproduced by $T_{\mathrm{i,L}}^{\mathrm{ref}}(r)$. The profile gain factor is evaluated to be $G_{1.0} = 0.987$, which is approximately unity as expected.

3.3. Analysis of the ion-ITB transition discharge

The profile gain factor is applied to the discharge # 136281 that involves dynamic formation of the ion-ITB. The time evolutions of the injected NB power and the line averaged density are shown in Fig. 2 (a). Before the ion-ITB transition starts, the plasma is sustained by three tangentially injected NBs (# 1-3) and one perpendicularly injected NB (# 5). Another perpendicular NB (# 4) is injected at $t = 4.6$ s, which seems to trigger the ITB transition. At the same time, the ion temperature measurement starts because the NB # 4 is the probe beam of the charge exchange recombination spectroscopy. This beam is modulated with 10 Hz and 80 % duty ratio for the background emission subtraction. In order to enhance the carbon impurity emission by the charge exchange recombination reaction from the core, a carbon pellet is injected before the NB # 4 starts, which is also considered to reduce the ion thermal transport. Figures 2 (b)-(d) show the spatiotemporal evolutions of the ion temperature, the ion temperature gradient, and the thermal diffusion coefficient, respectively. The central ion temperature continuously increases until $t \sim 4.75$ s. A strong gradient region emerges

at $t \sim 4.65$ s and $r_{\rm eff} \sim 0.3$ m, which drifts towards the core region. The thermal diffusivity is minimized at the radius where the gradient is strong, which corresponds to the ion-ITB formation. The ion-ITB gradually degrades after one of the tangentially injected NBs breaks down at $t \sim 4.8$ s, and finally the improved confinement region disappears. After $t = 5.1$ s, the power of the NB # 4 is halved, which results in a larger noise in the ion temperature measurement.

The reference L-mode profile $T_{\rm i,L}^{\rm ref}(r)$ is obtained by fitting the edge ion temperature profile with the L-mode profile function $T_{\rm i,L}(r|k)$ and by extrapolating it to the core. The spatiotemporal evolution of $T_{\rm i,L}^{\rm ref}(r)$ is shown in Fig. 2 (e). Although the core ion temperature drastically changes when the ITB is formed, the change in $T_{\rm i,L}^{\rm ref}(r)$ is moderate. Both the measured ion temperature profiles and the reference L-mode profiles at $t = 4.61$, 4.73, and 5.15 s are shown in Figs. 3 (a)-(c), respectively. These three time slices correspond to the initial measurement frame, the frame at which the central ion temperature is the maximum, and the frame after the ion-ITB has disappeared, respectively. In time slices Figs. 3 (a) and (c), the reference L-mode profiles are slightly lower than the measured ion temperature profiles, showing that the confinement improvement in those time frames are not significant. When the central ion temperature becomes the maximum, the deviation of the measured ion temperature profile from the reference L-mode profile is maximized, due to both increase of the measured ion temperature profile and decrease of the reference L-mode profile. The latter effect corresponds to the 'see-saw' effect, as discussed in [22]. The difference between the

measured ion temperature profile and the reference L-mode profile is quantified as the profile gain factor, Eq. (10), which is shown in Fig. 2 (f). The achieved central ion temperature $T_{\mathrm{i}0}$ and the central ion temperature of the reference L-mode profile $T_{\mathrm{i}0,\mathrm{L}}^{\mathrm{ref}}$ are also plotted in the same figure. It is shown that $T_{\mathrm{i}0}$ varies drastically while $T_{\mathrm{i}0,\mathrm{L}}^{\mathrm{ref}}$ remains almost unchanged. This difference is reflected in the change of the profile gain factor. At $t = 4.73$ s, $G_{1.0} \sim 1.5$ is obtained, clearly showing the strong ion-ITB formation. As the profile gain factor is the integrated quantity, it is robust against the noise. The value of the profile gain factor is stable even in $t > 5.1$ s in which the noise level in the ion temperature measurement increases, while the obtained diffusion coefficient becomes less smooth in space.

In the time instance at which the profile gain factor is the maximum, the conventional criterion of the ITB formation is performed for comparison. Figure 3 (d) shows the diffusion coefficient plotted as a function of the ion temperature for various radii at $t = 4.73$ s. In a large part of the radius, $r_{\mathrm{eff}} \geq 0.25$ m, the diffusion coefficient is decrementally scaled by the ion temperature, i.e., $\alpha < 0$. In these radii, the more the ion temperature evolves the better the thermal confinement becomes, violating the L-mode scaling of the diffusion coefficient. The red curve in Fig. 3 (d) corresponds to the T_{i}^{-1} dependence, showing a good agreement with the experimental data. It should be noted that this analysis is only applicable when T_{i} is measured with good quality, because the noise in evaluating $|\nabla T_{\mathrm{i}}|$ is directly reflected to χ_{i}.

One of the other criterions of the ITB, the relative gradient between the core and

the edge, $|\nabla T_{\mathrm{i,core}}|/|\nabla T_{\mathrm{i,edge}}|$ [17], is also evaluated and is compared with the profile gain factor. Since the ITB position changes in time, the core gradient is evaluated at three different radii, $r_{\mathrm{eff}} = 0.2$, 0.3, and 0.4 m, and the corresponding relative gradients are evaluated with respect to the edge gradient at $r_{\mathrm{eff}} = 0.5$ m. The time evolutions of the relative ion temperature gradients are shown in Fig. 2 (g). The ITB is formed at the edge first and then propagates inward. Therefore, the change in the relative gradient at the core side is delayed compared to that at the edge side. The magnitude of changes depend on the radius too, and in this case the relative gradient at $r_{\mathrm{eff}} = 0.2$ m evolves most drastically. It is shown that properties of the relative gradient strongly depend on space because it is a local parameter. Meanwhile the profile gain factor, which is an integrated scalar parameter, shows the overall characteristics of the ITB confinement improvement. The latter is beneficial for a wide range parameter scan study.

It is valuable to compare the ITB in LHD with that in tokamaks. In the JET device, the ion temperature profile is attributed to show an ITB when the dimensionless parameter

$$\rho^*_{T_\mathrm{i}} = \rho_\mathrm{s}/L_{T_\mathrm{i}}. \tag{11}$$

exceeds a critical value, i.e., $\rho^*_{T_\mathrm{i}} > \rho^*_{\mathrm{ITB}} = 0.014$ [9], where ρ_s is the drift wave scale length and $L_{T_\mathrm{i}} = -T_\mathrm{i}^{-1}\nabla T_\mathrm{i}$ is the gradient length of the ion temperature profile. The drift wave scale length is given as $\rho_\mathrm{s} = B_\mathrm{t}^{-1}\sqrt{T_\mathrm{e} m_\mathrm{i}/e}$, where m_i is the ion mass and e is the electron charge. This dimensionless parameter $\rho^*_{T_\mathrm{i}}$ is interpreted as an indicator of how strong the turbulence is stabilized by the $E \times B$ shear flows associated with large

pressure gradients and plasma rotation. In the case of LHD, $\rho^*_{T_\mathrm{i}}$ is slightly below 0.014 at maximum, showing that the ITB in LHD is as strong as the marginal ITB in JET. This difference of the ITB strength might originate from different saturation mechanism of the ion temperature profile in the L-mode. By use of the profile gain factor, the reference L-mode profile can be arbitrary set according to the L-mode scaling manner in different devices, which facilitates quantitative comparison between ITBs in tokamaks and stellarators/heliotrons. General differences in the ITB behaviors in tokamaks and stellarators/heliotrons are summarized in a review [2].

4. Summary

In this paper, a new criterion for the internal transport barrier formation was proposed by defining a unique scalar parameter, the profile gain factor. The profile gain factor showed degree of the confinement improvement with respect to an arbitrary reference temperature profile scaling in the L-mode. As the reference L-mode profile for LHD, the edge ion temperature profile data was extrapolated to the core by the L-mode profile function, which uses the thermal diffusion coefficient being proportional to the local ion temperature. The profile gain factor was defined as the ratio of the ion stored energy experimentally measured to that evaluated from the reference L-mode profile. The proposed method was applied to the LHD experimental data, and its capability for quantification of the ITB strength was demonstrated.

The proposed method in this paper can be applied for a large database with a

wide range parameter scan experiment. In particular, the ITB onset power threshold study [5, 7] is expected to be feasible for relatively weak ITBs in stellarators/heliotrons to understand underlying physics and to obtain better controllability. Future applied studies are anticipated.

Acknowledgments

The authors acknowledge all the members of the LHD Experiment Group for their assistance. The authors also thank Professors S. Sakakibara for strong support and useful discussions. This work is partly supported by the National Institute for Fusion Science grants (17KLPH031 and ULHH033) and by the Grant-in-Aid for Scientific Research of JSPS (17K14898).

Appendix

In this section, the computational scheme for solving the nonlinear diffusion equation is explained.

4.1. Finite differentiation

Here, the temperature profile $T(r)$ for any particle spicies is denoted as the combination of the temperature vector

$$\mathbf{T} = (T_1, T_2, \cdots, T_n) \tag{12}$$

and the flux surface coordinate vector

$$\mathbf{r} = (\Delta, 2\Delta, \cdots, n\Delta), \tag{13}$$

that has a regular separation of Δ. The thermal transport equation Eq. (4) is discretized with the central finite differences, i.e.,

$$\frac{\partial T_j}{\partial r} = \frac{T_{j+1} - T_{j-1}}{2\Delta} \tag{14}$$

and

$$\frac{\partial^2 T_j}{\partial r^2} = \frac{T_{j+1} - 2T_j + T_{j-1}}{\Delta^2} \tag{15}$$

for j-th component. The discretized version of Eq. (4) becomes the nonlinear simultaneous algebraic equation with n variables denoted as $f_j(\mathbf{T}) = 0$, where the subscript j represents the number of the equation. The l.h.s. of Eq. (4) is given as

$$f_j(\mathbf{T}) = kT_j^{\alpha}\left(l_{\mathrm{p}}T_{j+1} + l_{\mathrm{m}}T_{j-1}\right) - 2kT_j^{\alpha+1} + \frac{\alpha k T_j^{\alpha-1}}{4}\left(T_{j+1} - T_{j-1}\right)^2 + \frac{\Delta^2 P_j}{n_j}, \tag{16}$$

where

$$l_{\mathrm{p}} = 1 + \frac{\Delta}{2L} \tag{17}$$

and

$$l_{\mathrm{m}} = 1 - \frac{\Delta}{2L}. \tag{18}$$

By solving $f_j(\mathbf{T}) = 0$, the temperature profile $\mathbf{T}$ can be obtained.

4.2. Solving nonlinear simultaneous algebraic equation

Equation $f_j(\mathbf{T}) = 0$ is solved iteratively since it is a nonlinear equation. First, an initial profile $\mathbf{T}$ has to be found, which is not too far from the final solution. The initial profile

is renewed for aiming to make $\mathbf{f}(\mathbf{T})$ be closer to zero. Therefore, the new profile $\mathbf{T}+\delta\mathbf{T}$ is given so as to satisfy

$$\mathbf{f}(\mathbf{T}+\delta\mathbf{T})=0. \tag{19}$$

This equation is approximated by use of the Taylor expansion as

$$J(\mathbf{T})\delta\mathbf{T}=-\mathbf{f}(\mathbf{T}), \tag{20}$$

where $J(\mathbf{T})$ is the Jacobian matrix, from which $\delta\mathbf{T}$ can be obtained. The initial profile is updated by $\mathbf{T}+\delta\mathbf{T}$, and the iteration continues until the profile converges. For the actual application, the following modification is made,

$$\left[J(\mathbf{T})^{\mathrm{T}}J(\mathbf{T})+\lambda\mathbf{I}\right]\delta\mathbf{T}=-J(\mathbf{T})^{\mathrm{T}}\mathbf{f}(\mathbf{T}), \tag{21}$$

where λ is the tunable damping factor, in order to enhance the stability. At the initial stage of the iteration, the damping factor λ is set to be a larger value, by which the algorithm is made closer to the gradient-descent method. At the later stage, the damping factor is suppressed, which brings the method closer to the Newton algorithm. This procedure is known as the Levenberg-Marquardt method.

The Jacobian matrix is obtained by taking the derivative of Eq. (16) as

$$\frac{\partial f_j}{\partial T_j}=\alpha k T_j^{\alpha-1}\left(l_{\mathrm{p}}T_{j+1}+l_{\mathrm{m}}T_{j-1}\right)-2\left(\alpha+1\right)kT_j^{\alpha}+\frac{\alpha(\alpha-1)kT_j^{\alpha-2}}{4}\left(T_{j+1}-T_{j-1}\right)^2 \tag{22}$$

$$\frac{\partial f_j}{\partial T_{j+1}}=l_{\mathrm{p}}kT_j^{\alpha}+\frac{\alpha kT_j^{\alpha-1}}{2}\left(T_{j+1}-T_{j-1}\right) \tag{23}$$

$$\frac{\partial f_j}{\partial T_{j-1}}=l_{\mathrm{m}}kT_j^{\alpha}-\frac{\alpha kT_j^{\alpha-1}}{2}\left(T_{j+1}-T_{j-1}\right) \tag{24}$$

$$\frac{\partial f_j}{\partial T_i}=0 \qquad \text{when } i\notin\{j-1,j,j+1\} \tag{25}$$

To solve the nonlinear simultaneous algebraic equation, the boundary conditions must be given at both sides. Here, simply $T_0 = T_1$ is given for the core side and $T_{n+1} = T_{\mathrm{edge}}$ is given for the edge side, where T_{edge} is obtained from the measured profile at $r = (n+1)\Delta$. When $j = 1$, Eq. (22) becomes

$$\frac{\partial f_1}{\partial T_1} = \alpha k T_1^{\alpha-1}\left(l_{\mathrm{p}} T_2 + l_{\mathrm{m}} T_1\right) - 2\left(\alpha+1\right) k T_1^{\alpha} + \frac{\alpha(\alpha-1) k T_1^{\alpha-2}}{4}\left(T_2 - T_1\right)^2 + k l_{\mathrm{m}} T_1^{\alpha} - \frac{\alpha k T_1^{\alpha-1}}{2}\left(T_2 - T_1\right). \tag{26}$$

The iteration procedure is terminated when the profile is converged. Whether the profile is converged is judged by use of the history of the profile update. It is defined as

$$\epsilon^i = \sqrt{\sum \Delta \mathbf{T}^2 / \sum \mathbf{T}^2}, \tag{27}$$

where $\Delta\mathbf{T}$ is the difference between i-th profile and $(i-1)$-th profile and the sum is taken over radii which are subject to the analysis. When ϵ^i becomes below a certain threshold value, the iteration process is stopped and the profile is regarded as the final solution.

4.3. Initial profile

By substituting $\alpha = 0$ to the equations, the nonlinearity disappears and the equations can be uniquely solved without using iteration. Now the equations to be solved are

$$J\mathbf{T}^{\mathrm{T}} = -\frac{\Delta^2 P_j}{n_j}. \tag{28}$$

The Jacobian matrix becomes independent of $\mathbf{T}$ as

$$\frac{\partial f_j}{\partial T_j} = -2k, \tag{29}$$

$$\frac{\partial f_j}{\partial T_{j+1}} = l_{\mathrm{p}} k, \tag{30}$$

$$\frac{\partial f_j}{\partial T_{j-1}} = l_{\mathrm{m}} k, \tag{31}$$

and

$$\frac{\partial f_j}{\partial T_i} = 0 \qquad \text{when } i \notin \{j-1, j, j+1\}. \tag{32}$$

When $j = 1$, Eq. (29) becomes

$$\frac{\partial f_1}{\partial T_1} = -\left(2 - l_{\mathrm{m}}\right) k \tag{33}$$

For other elements, $T_0 = T_1$ and $T_{n+1} = T_{\mathrm{edge}}$ are substituted in the equations when $j = 1$ and $j = n$, respectively. The solution is used as the initial value for the iteration.

4.4. Numerical test

Capability of the proposed method is examined numerically. We provide the test parameters as $k = 2$ and $\alpha = 1$, and attempt to solve the nonlinear thermal transport equation. Radial profiles of the density and the heating power density are given as shown in Fig. 4 (a). Here, according to the typical NB sustained discharge in LHD, we employ the flat density profile and the centrally peaked heating power density profile. The results of the calculation are also shown in Figure 4 (a), in which all the history of the iteration is over plotted. The iteration converges at the seventh step. At the initial stage, the thermal transport equation is pure diffusion equation with the constant diffusion coefficient $\chi = k$ m^2/s. Because the diffusion coefficient is constant, a centrally peaked temperature profile is obtained owing to the centrally peaked heating profile. As the

iteration stage progresses, the profile approached to the final profile without diverging. In the final iteration stage, the temperature profile becomes the dome-like shape having the minimum gradient at the core and the maximum gradient at the edge, i.e., the more the temperature increases the worse the confinement becomes.

It is essential to examine how the diffusion coefficient depends on the temperature. The diffusion coefficient, i.e., the heat flux normalized by the density and the temperature gradient, is plotted as a function of the temperature in Fig. 4 (b). In the case of the initial profile, the diffusion coefficient is constant with respect to the temperature, except for the very core region and very edge region, in which the boundary conditions affect the profile. Meanwhile, in the case of the final profile, the diffusion coefficient is proportional to T^1, showing that the final profile satisfies Eq. (3) with the given parameters k and α.

References

[1] R C Wolf 2002 *Plasma Phys. Control. Fusion* **45** R1

[2] K Ida and T Fujita 2018 *Plasma Phys. Control. Fusion* **60** 033001

[3] F Wagner 2007 *Plasma Phys. Control. Fusion* **49** B1

[4] T Fujita, S Ide, H Shirai, M Kikuchi, O Naito, Y Koide, S Takeji, H Kubo, and S Ishida 1997 *Phys. Rev. Lett.* **78** 2377

[5] C Gormezano 1999 *Plasma Phys. Control. Fusion* **41** B367

[6] E J Doyle, G M Staebler, L Zeng, T L Rhodes, K H Burrell, C M Greenfield, R J Groebner, G R McKee, W A Peebles, C L Rettig, *et al* 2000 *Plasma Phys. Control. Fusion* **42** A237

[7] Y Koide, T Takizuka, S Takeji, S Ishida, M Kikuchi, Y Kamada, T Ozeki, Y Neyatani, H Shirai, M Mori, *et al* 1996 *Plasma Phys. Control. Fusion* **38** 1011

[8] A G Peeters, O Gruber, S Günter, M Kaufmann, H Meister, G V Pereverzev, F Ryter, A C C Sips, J Stober, W Suttrop, *et al* 2002 *Nucl. Fusion* **42** 1376

[9] G Tresset, X Litaudon, D Moreau, X Garbet, *et al* 2002 *Nucl. Fusion* **42** 520

[10] F Ryter, F Imbeaux, F Leuterer, H-U Fahrbach, W Suttrop, and ASDEX Upgrade Team 2001 *Phys. Rev. Lett.* **86** 5498

[11] P Mantica, D Strintzi, T Tala, C Giroud, T Johnson, H Leggate, E Lerche, T Loarer, AG Peeters, A Salmi, *et al* 2009 *Phys. Rev. Lett.* **102** 175002

[12] F Wagner, O Gruber, K Lackner, HD Murmann, E Speth, G Becker, HS Bosch, H Brocken, G Cattanei, D Dorst, *et al* 1986 *Phys. Rev. Lett.* **56** 2187

[13] H Yamada, S Murakami, K Yamazaki, O Kaneko, J Miyazawa, R Sakamoto, KY Watanabe, K Narihara, K Tanaka, S Sakakibara, *et al* 2003 *Nucl. Fusion* **43** 749

[14] K Ida, S Inagaki, T Shimozuma, N Tamura, H Funaba, K Narihara, S Kubo, S Murakami, A Wakasa, M Yokoyama, *et al* 2004 *Phys. Plasmas* **11** 2551–2557

[15] S Inagaki, H Takenaga, K Ida, A Isayama, N Tamura, T Takizuka, T Shimozuma, Y Kamada,

S Kubo, Y Miura, *et al* 2005 *Nucl. Fusion* **46** 133

[16] K Ida, S Inagaki, R Sakamoto, K Tanaka, H Funaba, Y Takeiri, K Ikeda, C Michael, T Tokuzawa, H Yamada, *et al* 2006 *Phys. Rev. Lett.* **96** 125006

[17] K Nagaoka, Y Takeiri, K Ida, M Yoshinuma, S Morita, N Tamura, T Ido, A Shimizu, K Ikeda, M Osakabe, *et al* 2010 *Plasma Fusion Res.* **5** S2029–S2029

[18] H Yamada, K Kawahata, T Mutoh, N Ohyabu, Y Takeiri, S Imagawa, K Ida, T Mito, Y Nagayama, T Shimozuma, *et al* 2010 *Fus. Sci. Technol.* **58** 12–28

[19] M Yoshinuma, K Ida, M Yokoyama, M Osakabe, and K Nagaoka 2010 *Fus. Sci. Technol.* **58** 375–382

[20] I Yamada, K Narihara, H Funaba, T Minami, H Hayashi, T Kohmoto, and LHD Experiment Group 2010 *Fus. Sci. Technol.* **58** 345–351

[21] S Murakami, H Yamaguchi, A Sakai, A Wakasa, A Fukuyama, K Nagaoka, H Takahashi, H Nakano, M Osakabe, K Ida, *et al* 2015 *Plasma Phys. Control. Fusion* **57** 054009

[22] K Ida, M Yoshinuma, K Nagaoka, M Osakabe, S Morita, M Goto, H Funaba, M Yokoyama, K Ikeda, H Nakano, *et al* 2010 *Contrib. Plasma Phys.* **50** 558–561

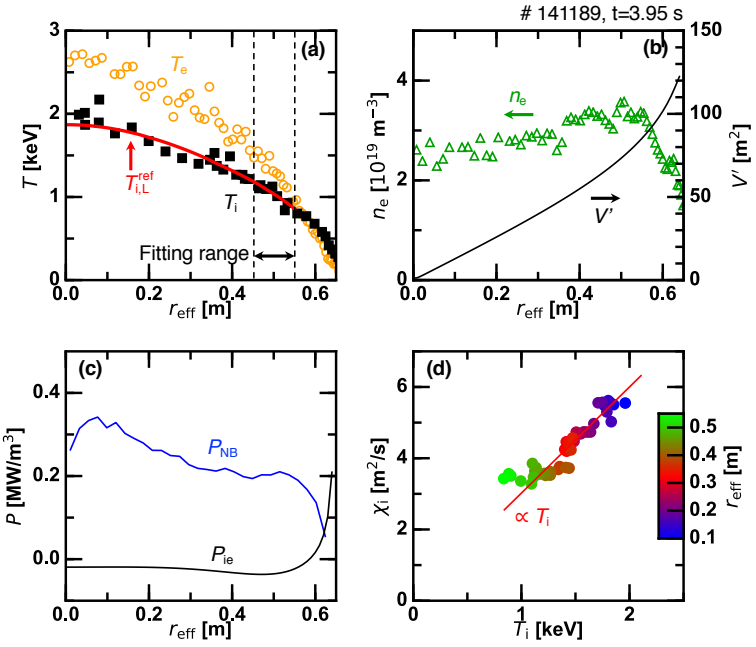

Figure 1. Radial profiles of the typical L-mode discharge; (a) ion temperature, the electron temperature, and the reference L-mode profile, (b) the electron density and the partial derivative of the torus volume, and (c) the heating power density by the NBs and the electron-ion energy exchange ratio. (d) Heat diffusion coefficient as a function of the ion temperature. The fitting range is shown in (a).

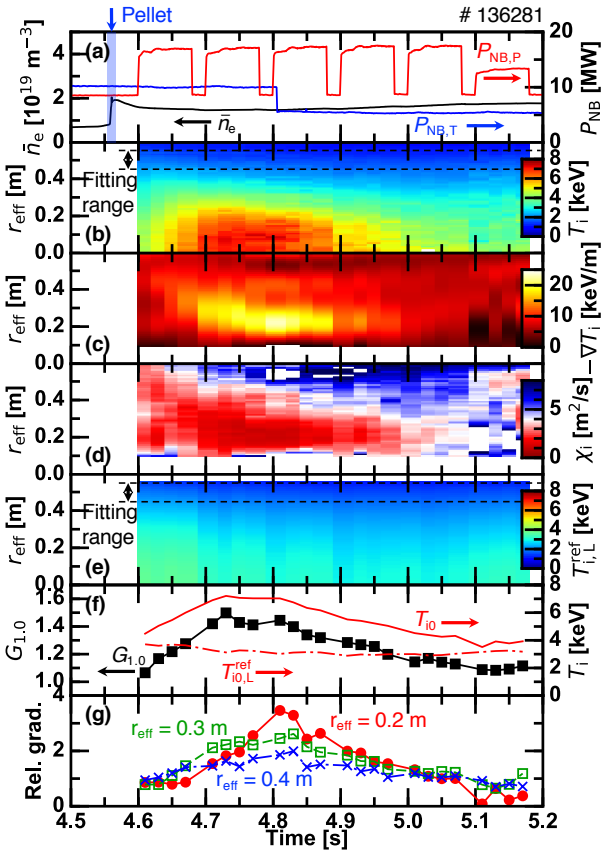

Figure 2. Time evolutions of (a) the heating scenario and the line averaged density, (b) the ion temperature profile, (c) the ion temperature gradient profile, (d) the heat diffusion coefficient profile, (e) the reference L-mode profile, (f) the central ion temperature, the extrapolated central ion temperature, and the profile gain factor with $\alpha = 1$, and (g) the relative ion temperature gradient with respect to $r_{\rm eff} = 0.5$ m. The fitting range is shown in (b) and (e).

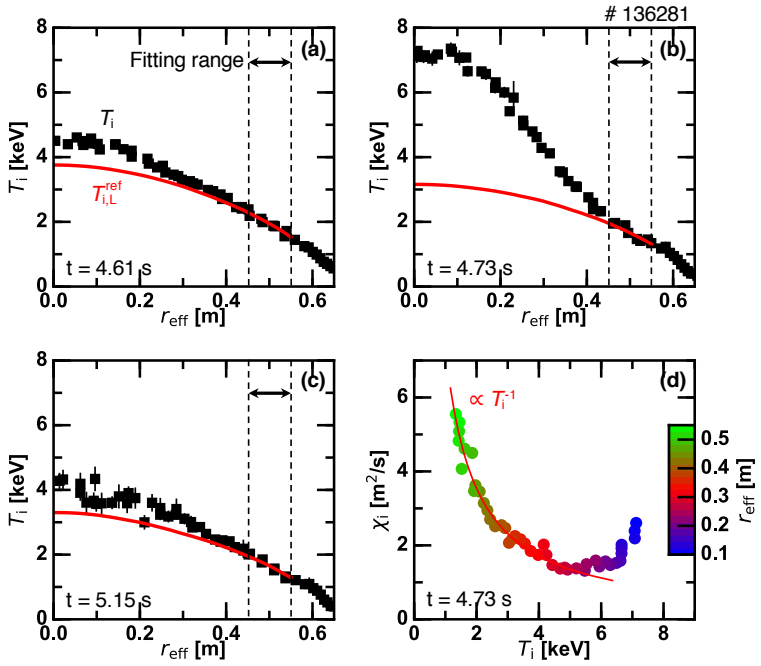

Figure 3. (a-c) Measured ion temperature profiles and the reference L-mode profiles at $t = 4.61$ s, 4.73 s, and 5.15 s, respectively. (d) Heat diffusion coefficient as a function of the ion temperature at $t = 4.73$ s. The fitting range is shown in (a)-(c).

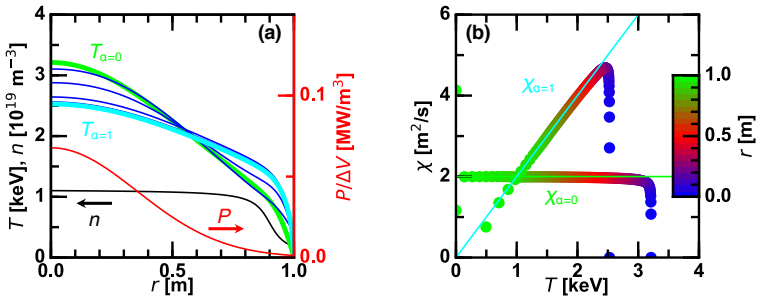

Figure 4. (a) Radial profiles of the density profile and the heating power density profile given as test data and the history of the temperature profile derivation. The initial profile ($\alpha = 0$) and the final profile ($\alpha = 1$) are shown by the green and light blue thick curves, respectively, while the history between them is shown by the blue thin curves. (b) Diffusion coefficient as a function of temperature when $\alpha = 0$ and $\alpha = 1$.